



## GPS autoproteolysis is required for CD97 to up-regulate the expression of N-cadherin that promotes homotypic cell–cell aggregation

Cheng-Chih Hsiao, Hsin-Yi Chen, Gin-Wen Chang, Hsi-Hsien Lin \*

Department of Microbiology and Immunology, College of Medicine, Chang Gung University, 259 Wen-Hwa 1st Road, Kwei-San, Tao-Yuan, Taiwan

### ARTICLE INFO

#### Article history:

Received 24 August 2010  
Revised 22 November 2010  
Accepted 6 December 2010  
Available online 13 December 2010

Edited by Lukas Huber

#### Keywords:

CD97  
Homotypic cell–cell aggregation  
N-cadherin  
Epidermal growth factor module-containing seven-transmembrane receptor  
GPCR proteolysis site autoproteolysis  
G protein-coupled receptor

### ABSTRACT

**Most adhesion-class G protein-coupled receptors (adhesion-GPCRs) undergo a novel self-catalytic cleavage at the GPCR proteolysis site (GPS) to form a hetero-dimeric complex containing the extra-cellular and seven-span transmembrane subunits. However, little is known about the role of GPS auto-proteolysis in the function of adhesion-GPCRs. Here we show that GPS cleavage is essential for the homotypic cell aggregation promoted by CD97 receptor, a leukocyte-restricted adhesion-GPCR often aberrantly expressed in carcinomas. We find that CD97 does not mediate cell aggregation directly. Instead, expression of the wild type – but not the GPS cleavage-deficient CD97 up-regulates the expression of N-cadherin, leading to Ca<sup>2+</sup>-dependent cell–cell aggregation. Our results provide a clear evidence for the role of GPS proteolytic modification in the cellular function of adhesion-GPCRs.**

© 2010 Federation of European Biochemical Societies. Published by Elsevier B.V. All rights reserved.

### 1. Introduction

As the second largest G protein-coupled receptor (GPCR) sub-family in the human proteome, the adhesion-GPCRs [1] have been shown to play an important role in the recognition and uptake of apoptotic cells [2], metastasis of melanoma cells [3], the normal development of brain cortex [4], the control of tissue polarity and morphogenesis [5,6], the normal auditory and visual function [7], male fertility [8], and the immune regulation [9].

Adhesion-GPCRs are characterized by the chimeric composition of a long ectodomain (ECD) and a seven-span transmembrane (7TM) region [10]. A unique post-translational modification by self-catalytic cleavage at the GPCR proteolysis site (GPS) dissects the receptor into the ECD- and 7TM-subunits [11]. The two resultant subunits are thought to associate non-covalently on the cell surface as a receptor complex. However, recent results suggested that it is also possible for the two subunits to behave independently as separate protein entities [12,13]. GPS auto-proteolysis

has been shown as a prerequisite for efficient surface trafficking of some but not all adhesion-GPCRs [11,14,15]. Furthermore, mutations that impair GPS cleavage are linked to human genetic disorders [4,16]. Thus, GPS auto-proteolysis is considered as an essential step for the functional maturation of adhesion-GPCRs. However, a link between the GPS proteolysis and the cellular functions of adhesion-GPCRs has not been systemically investigated.

In this report, we aim to evaluate the role of GPS proteolysis in the cellular function of CD97. CD97 was first identified as an early activation marker of lymphocytes [17–19]. Later, it was found to be expressed restrictedly in cells of myeloid and lymphoid lineages and smooth muscle cells. Aberrant expression of CD97 was also often identified in various carcinoma cells and tissues [20]. CD97 belongs to the epidermal growth factor module-containing seven-transmembrane receptor sub-group of adhesion-GPCR family and contains a total of 5 epidermal growth factor (EGF)-like motifs in the N-terminal ECD [21,22]. Alternative mRNA splicing generated three major CD97 isoforms that contain different combinations of EGF-like motifs, including CD97(125), CD97(1235), and CD97(1-5) [18]. Recent studies have identified several specific cellular ligand(s) that interact with CD97 either in an isoform-dependent or -independent fashion. Thus, CD55 binds strongly to CD97(125) but weakly to CD97(1235) and CD97(1-5) [23]; chondroitin sulfate binds only to CD97(1-5) [24];  $\alpha 5\beta 1$  and  $\alpha v\beta 3$  integrins bind to all CD97 isoforms via a RGD motif in the stalk region [25].

*Abbreviations:* 7TM, seven-transmembrane; ECD, ectodomain; EDTA, 2,2',2'',2'''-(ethane-1,2-diyl)dinitrilo)tetraacetic acid; EGF-TM7, epidermal growth factor module-containing seven-transmembrane receptor; EGTA, glycol-bis(2-aminoethyl ether)-N,N,N',N'-tetraacetic acid; Fc, fragment crystallisable; GPCR, G protein-coupled receptor; GPS, GPCR proteolysis site; WT, wild-type

\* Corresponding author. Fax: +886 3 2118469.

E-mail address: [hlin@mail.cgu.edu.tw](mailto:hlin@mail.cgu.edu.tw) (H.-H. Lin).

Functional studies using specific Abs, recombinant CD97 proteins, and knock-out animals have revealed a role for CD97 in leukocyte migration, recruitment and activation [26–29]. In addition, CD97 is known to be involved in angiogenesis and the migration and invasion of tumor cells [20,25,30]. In this report, we show that GPS auto-proteolysis is required for CD97 to promote cell aggregation in HT1080 cells. The expression of a functional CD97 receptor up-regulates the expression of N-cadherin and its associated intracellular adaptors, leading to Ca<sup>++</sup>-dependent homotypic cell–cell aggregation. This is one of the first reports linking the GPS proteolytic modification and the cellular function of an adhesion-PCR.

## 2. Materials and methods

### 2.1. Reagents and cell culture

General chemicals were of analytical grade and obtained from Sigma, unless otherwise stated. CLB/CD97-1 mAb (mouse IgG2a) was purchased from AbD Serotec (Kidlington, UK). CLB/CD97-3, 2A1 and 2B1 mAbs were gifts from Dr. Jörg Hamann (University of Amsterdam, The Netherlands). Function-blocking anti-integrin mAbs from Millipore (Temecula, CA) are anti- $\alpha$ 2 (clone P1E6), anti- $\alpha$ V $\beta$ 3 (clone LM609), anti- $\alpha$ V $\beta$ 5 (clone P1F6), and anti- $\beta$ 1 (clone P4C10). Blocking (clone IIA1) and non-blocking (clone VC5) anti- $\alpha$ 5 Abs and anti C-terminal N-cadherin (clone 32/N-cadherin) Abs were from BD Biosciences (San Jose, CA). Mouse isotype control Ab and  $\beta$ -catenin (clone 7F7.2) mAb were purchased from R&D system (Minneapolis, MN) and Millipore, respectively. Anti- $\alpha$ -catenin (clone 1G5) and anti-p120 catenin (H-90) were obtained from Santa Cruz (Delaware Avenue, CA). Anti N-terminal N-cadherin mAb (clone GC-4) and Horseradish peroxidase (HRP)-conjugated secondary Ab were acquired from Sigma. All culture media were from Invitrogen and were supplemented with 10% heat inactivated fetal calf serum (FCS), 2 mM L-glutamine, 50 IU/ml penicillin and 50  $\mu$ g/ml streptomycin. HT1080 cells were cultured in Minimum Essential Medium (MEM) containing non-essential amino acids and 1 mM sodium pyruvate. HEK-293T was cultured in Dulbecco's Modified Eagle Medium (DMEM). Purified CD97 (1-5)-mFc, CD97 (125)-mFc, EMR2 (125)-mFc and mFc have been described previously [31].

### 2.2. Construction of expression vectors

The retroviral expression constructs were generated using the pFB-Neo vector (Stratagene, La Jolla, CA). The wild type (WT) and S531A mutant of CD97 (125) and CD97(1-5) isoforms were amplified by PCR using respective templates. Primers (CD97-Sal I-5: 5'-ata aag tcc tgg cct gtc gac agc ctg cac agc tgc-3') and (CD97-Not I-3: 5'-tgg gcc gtc cag aag cgg ccg cct tca tat gcc-3') were used to generate the cDNA inserts to clone into the pFB-Neo vector via the Sal I and Not I sites.

### 2.3. Retroviral infection and selection of stable cell lines

HEK-293T packaging cells in 100-mm dishes were transfected with 3  $\mu$ g each of the pFB-Neo expression construct, pVPack-VSV-G and pVPack-GP vectors (Stratagene) plus 50  $\mu$ l of Lipofectamine<sup>TM</sup> in Opti-MEM medium, as recommended by the supplier. Virus-containing supernatants were harvested 48 hr post-transfection, to which a final concentration of 5  $\mu$ g/ml polybrene solution was added. HT1080 cells (~40–50% confluence) in 6-well plates were infected with 1 ml of viral supernatants. Cells were spun for 90 min at 25 °C at 600 $\times$ g, followed by the addition of 2 ml of fresh complete medium 3 h later. The infected cells were then incubated for an additional 24 h at 37 °C before selection in medium contain-

ing 1 mg/ml G418. G418-resistant cells were collected after ~2 weeks of selection and confirmed by appropriate analysis. Cell proliferation assays were performed using the CellTiter<sup>®</sup> 96 Aqueous One solution assay (Promega, WI, USA) according to the manufacturer's instructions. Cells (1  $\times$  10<sup>3</sup> cells/well) were seeded in a 96-well plate at day 0 and cell growth measured everyday for 6 days with medium replenishment at day 3.

### 2.4. Cell aggregation assay

Cells were serum-starved for 20 h before harvesting in PBS/2 mM 2,2',2'',2'''-(ethane-1,2-diyldinitrilo)tetraacetic acid (EDTA) and resuspended at 5  $\times$  10<sup>5</sup> cells/ml in serum-free medium/5% BSA. Cells (100  $\mu$ l/well) were incubated in 96-well plates for 1 h at 37 °C, fixed with 1% formaldehyde and the number of single cells was counted with a hemocytometer. The extent of cell aggregation was determined using the equation:  $(1 - N1/N0) \times 100\%$ , where N0 is the number of single cells at the start of the experiment and N1 is the number of single cells after 1 h incubation. When necessary, various reagents such as cation chelators (EDTA and glycol-bis(2-aminoethylether)-N,N,N',N'-tetraacetic acid (EGTA), 5 mM), antibodies (5–150  $\mu$ g/ml), and soluble proteins (5–10  $\mu$ g/ml) were pre-incubated with cells for 15 min on ice before cell aggregation assay.

### 2.5. RT-PCR analysis and quantitative real time PCR

To identify N-cadherin,  $\beta$ -catenin and E-cadherin RNA transcripts, semi-quantitative RT-PCR and quantitative real time PCR (qRT-PCR) were performed using the iCycle system (Bio-Rad, CA, USA). In brief, total RNA was isolated using Trizol reagents (Invitrogen). 1  $\mu$ g of DNA-free total RNAs were reverse transcribed using oligo-dT<sub>(12–18)</sub> and MMLV reverse transcriptase as described previously [9]. For the semi-quantitative RT-PCR assay, cDNA products amplified by the specific primers (Supplementary Table 1) were separated by electrophoresis in 1% agarose gels. For the qRT-PCR assay, 25  $\mu$ l reaction containing 2  $\mu$ l cDNA, 0.3  $\mu$ M of each primer and 12.5  $\mu$ l Maxima<sup>TM</sup> SYBR Green qPCR Master Mix (Fermentas, Canada) was used to monitor double-strand DNA synthesis. qRT-PCR was carried out following the recommended thermal profile: 95 °C for 10 min (initial denaturation), followed by 40 cycles of 95 °C for 15 s (denaturation) and 60 °C for 1 min (annealing/elongation). Fluorescence intensity of the amplified products was measured at the end of each PCR cycle. Results of qRT-PCR were collected and analyzed by iQ<sup>TM</sup>5 Optical System Software (Bio-Rad, CA, USA). The end results of N-cadherin mRNA expression were normalized to internal control GAPDH mRNA.

### 2.6. Western blotting and flow cytometry analysis

For Western blotting, total cell lysates were separated in 8% or 10% SDS-PAGE gels, blotted and probed with specific primary Abs at optimal concentrations. Following extensive wash, blots were sequentially incubated with HRP-conjugated secondary Abs and ECL for detection. Flow cytometric analyses were carried out using standard procedures as described previously [14]. Briefly, cells were harvested and fixed with 4% paraformaldehyde at room temperature for 15 min. Cells were blocked in PBS containing 4% normal goat serum and 1% BSA (blocking buffer) for 30 min and then stained with appropriate 1<sup>st</sup> and 2<sup>nd</sup> Abs in blocking buffer, all at 4 °C. Cells were collected and analyzed on FACSscan using the flowjo software.

### 2.7. Statistical analysis

All experiments were performed at least three times. Results are shown as the mean  $\pm$  S.E.M., and comparisons were made using Student's *t*-test. A probability (*P*) of  $\leq 0.05$  is considered significant.

### 3. Results and discussion

#### 3.1. Generation of HT1080 cell lines stably expressing wild-type and GPS cleavage-deficient CD97 isoforms

To investigate the role of GPS auto-proteolysis in CD97-mediated cellular function, we established stable HT1080 cell lines expressing CD97(125)WT, CD97(125)S531A, CD97(1-5)WT, and CD97(1-5)S531A isoforms using a retroviral expression system (Fig. 1A). The CD97(125)WT and CD97(1-5)WT isoforms represented two major alternatively-spliced CD97 gene products containing the EGF-like domains 1-2-5 and 1-2-3-4-5, respectively. The S531A mutant was chosen because the single Ser to Ala mutation at the GPS site renders the receptor deficient in cleavage, but has no adverse effect on receptor expression (unpublished results). As revealed by the flow cytometry analysis, pFB-Neo vector-transduced HT1080 cells show a basal expression of CD97, while all stable cell lines display upregulated CD97 expression at a comparable level (~10-fold over the basal) (Fig. 1B). 2A1 mAb that recognizes a related adhesion-GPCR, EMR2, shows no expressional changes in all cell lines, confirming the specific over-expression of CD97. Western blot analysis using CD97/1 mAb that recognizes the first EGF-like domain identifies specific bands corresponding to the respective isoforms (1-5WT, ~85 kDa; 125WT, ~65 kDa; 1-5S531A, ~110 kDa; 125S531A, ~90 kDa) (Fig. 1C). A faint band of ~80–85 kDa representing endogenous CD97 molecules was detected in the parental and vector-transfected HT1080 cells (Fig. 1C). Thus, we confirm CD97(125)WT and CD97(1-5)WT are fully cleaved, while CD97(125)S531A and CD97(1-5)S531A are not proteolytically processed. All stable cell lines are found to be similar to the parental cells in the growth rate and cell morphology (Fig. 1C and Supplementary Fig. S1).

#### 3.2. A role for GPS auto-proteolysis in regulating homotypic cell aggregation by CD97

Although these cell lines are characteristically similar in normal culture conditions, we found that serum-starved CD97(125)WT and CD97(1-5)WT stable cells tended to aggregate faster and form much larger aggregates in comparison to the control and CD97S531A-expressing cells (Fig. 2A). Quantitative analysis showed that CD97WT stable cells display a ~91% degree of aggregation, while control cells and CD97S531A-expressing cells only reach ~50–60% degree of aggregation (Fig. 2B). These results suggest that GPS proteolytic modification is absolutely required for the expression of a functional CD97 receptor to promote homotypic cell–cell aggregation.

#### 3.3. CD97 upregulates the expression of N-cadherin, which promote HT1080 cell aggregation

We next investigate the mechanism whereby the expression of WT CD97 in HT1080 cells promotes homotypic cell aggregation. As an adhesion-GPCR, many cellular ligands including CD55, chondroitin sulfate, and  $\alpha 5\beta 1$  and  $\alpha v\beta 3$  integrins, have been identified for CD97 [23–25]. It is possible that interaction of CD97 with some of these ligand(s) leads to enhanced cell aggregation. Alternatively, cell aggregation could be induced secondarily as a result of WT CD97 expression in HT1080.

We first evaluate whether CD97 itself can mediate cell aggregation directly. Interestingly, addition of anti-CD97 Abs, soluble CD97-mFc proteins and various anti-integrin Abs all fail to inhibit cell aggregation even at high concentrations (Fig. 3). These data suggest that CD97 is not involved directly in mediating cell aggregation. This result prompts us to consider whether the expression

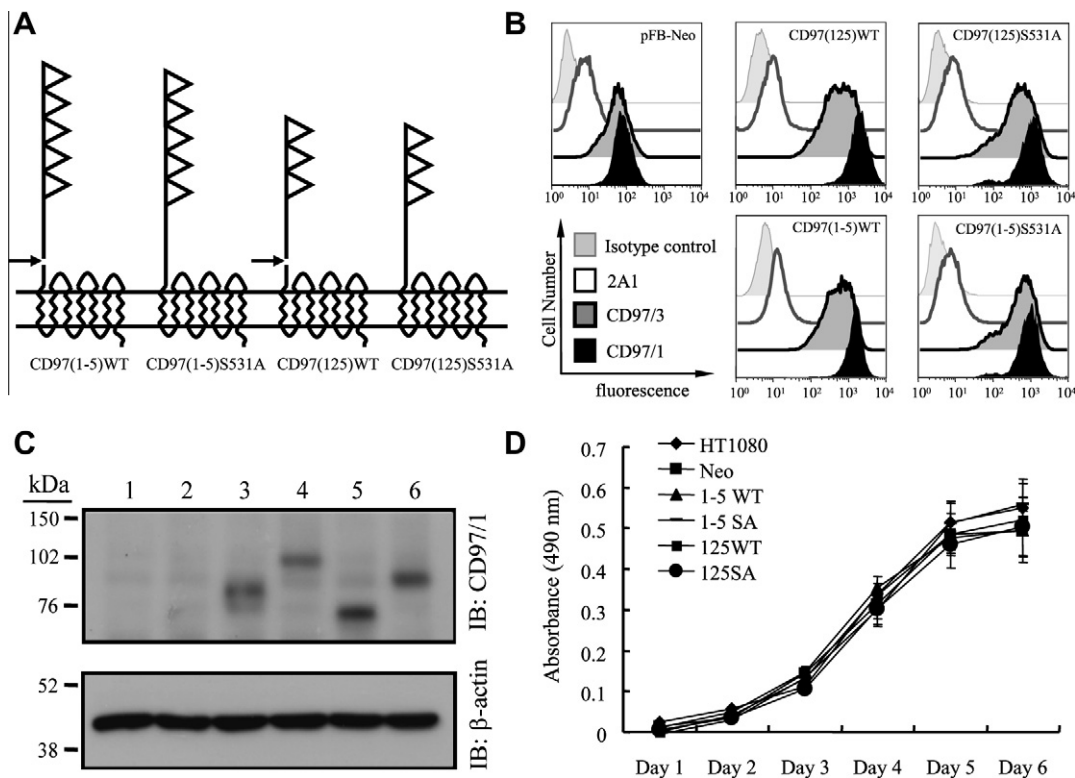


**Fig. 1.** Generation and characterization of HT1080 cell lines stably expressing CD97 isoforms with normal or defective GPS cleavage. (A) Schematic representation of CD97 isoforms. The triangles represent the EGF-like domains. The arrow indicates the GPS site. (B) Flow cytometry analysis of cell surface CD97 expression was performed using appropriate mAbs as indicated. (C) Western blot analysis verified the cleaved and uncleaved CD97 proteins in total cell lysate of parental HT1080 cells (lane 1), cells transduced by pFB-Neo vector only (lane 2), or vectors expressing CD97(1-5)WT (lane 3), CD97(1-5)S531A (lane 4), CD97(125)WT (lane 5), and CD97(125)S531A (lane 6) isoforms. (D) Cell growth analysis of the stable HT1080 cell lines. Data are means  $\pm$  S.E.M. of 3 independent experiments performed in triplicate.

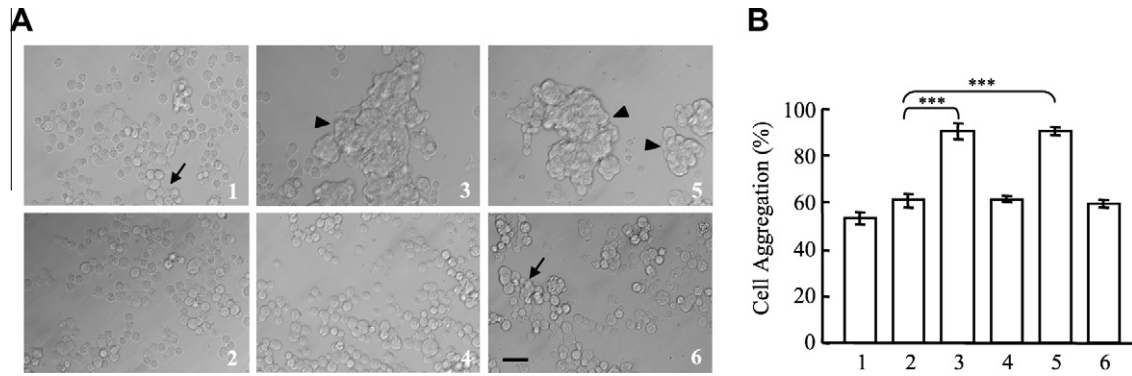


**Fig. 2.** GPS auto-proteolysis is essential for CD97 to promote HT1080 cell aggregation. (A and B) Serum-starved single cell suspension was incubated for 1 h at 37 °C. Cell aggregation was represented either by the microscopy observation (A) or by the measurement of the degree of aggregation (B) as described in "Section 2". The numbers 1–6 represent control and stable HT1080 cell lines as indicated in Fig. 1C. Large cell aggregates (arrowhead) were readily observed in cells over-expressing CD97-WT isoforms (panels 3 and 5), while much smaller aggregates (arrow) were found in control cells (panels 1 and 2) and cells expressing GPS cleavage-defective CD97 isoforms (panels 4 and 6). Data in B are means  $\pm$  S.E.M. of 4 independent experiments performed in triplicate. \*\*\* $P < 0.005$  compared to the control.

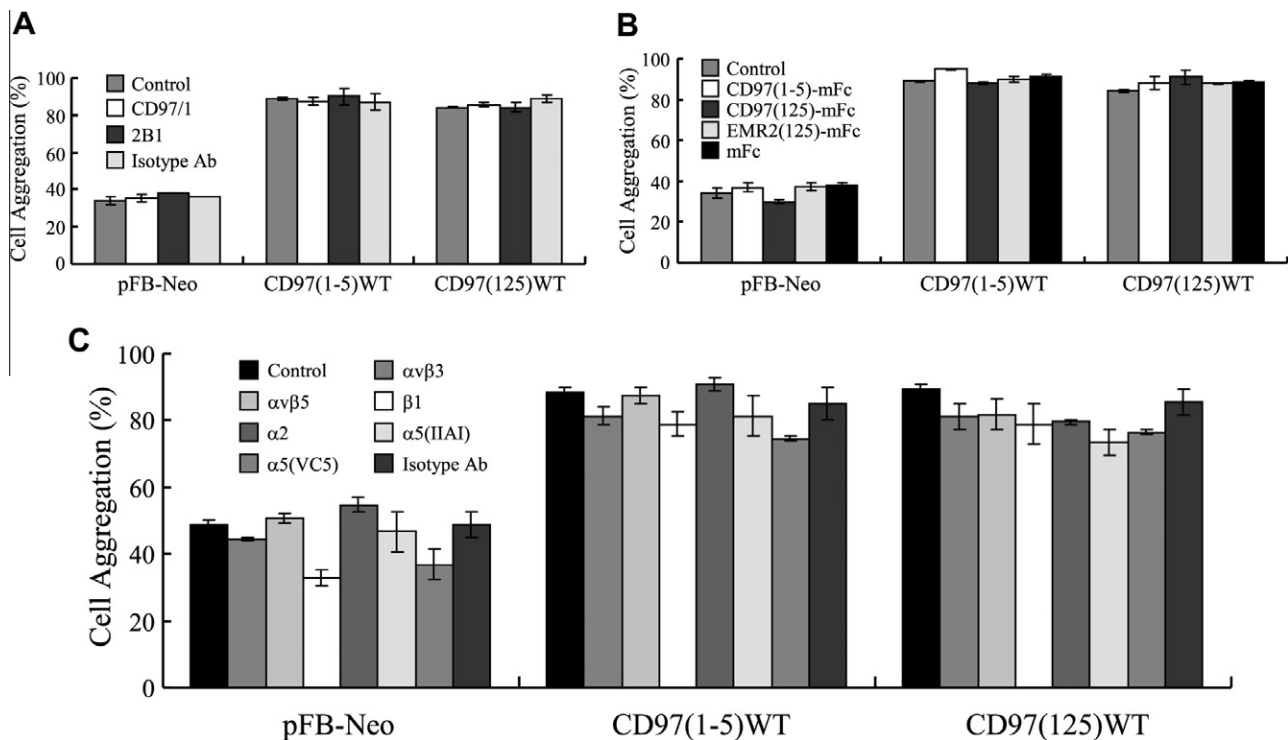


**Fig. 3.** CD97 does not mediate cell aggregation directly. Cell aggregation was analyzed on control and two CD97 WT stable HT1080 cells in the presence of (A) isotype control and anti-CD97 mAbs; (B) soluble CD97 protein isoforms and control proteins; (C) isotype control and anti-integrin mAbs all at 10  $\mu\text{g}/\text{ml}$  as indicated. Data are means  $\pm$  S.E.M. of 3 independent experiments performed in triplicate.

of WT CD97 in HT1080 somehow modulates cellular phenotypes to promote cell aggregation.

The cell aggregation seen here is reminiscent of the homotypic cell–cell adhesion mediated by members of the cadherin-superfamily such as E-cadherin and N-cadherin [32]. RT-PCR analysis shows that while no E-cadherin transcripts are ever detected in these cells, N-cadherin is indeed expressed in parental HT1080 cells. (Fig. 4A). Importantly, both semi-quantitative RT-PCR and real-time qRT-PCR analysis reveal a  $\sim 1.5$ -fold increase of N-cadherin transcript in cells expressing CD97WT isoforms in comparison to the vector control cells and CD97S531A-expressing cells (Fig. 4A and Supplementary Fig. S2).

Next, the level of cell surface N-cadherin is determined by flow cytometry. Again, CD97WT stable cells are found to display  $\sim$ two-

fold more N-cadherin than do control cells and CD97S531A-expressing cells in serum-starved and, to a less extent, in normal culture conditions (Fig. 4B and Supplementary Fig. S3). Finally, Western blot analysis revealed an increased expression of N-cadherin as well as  $\beta$ -catenin and  $\alpha$ -catenin, two downstream adaptors of N-cadherin, in CD97WT cells (Fig. 4C) [32]. Interestingly, the expression of p120-catenin, another N-cadherin adapter, seems to be compatible in all cell lines. These results indicate that expression of CD97WT, but not CD97S531A isoforms increases specifically the expression of N-cadherin and some of its adapter proteins.

N-cadherin mediates homotypic cell–cell adhesion in a  $\text{Ca}^{++}$ -dependent manner [32]. We therefore examine HT1080 cell aggregation in the presence of divalent cation chelators (EDTA and



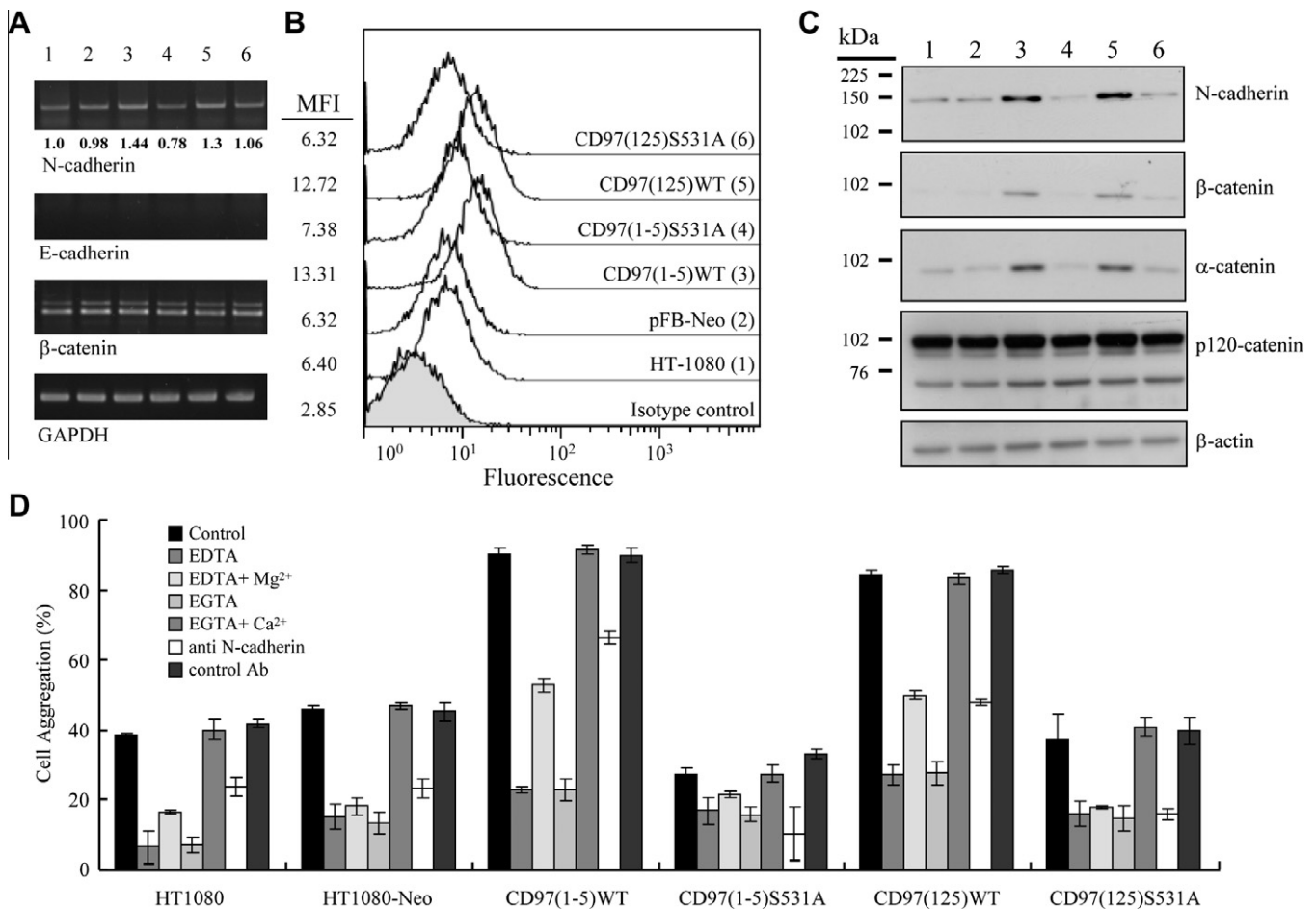


**Fig. 4.** Expression of CD97 WT isoforms upregulates the expression of N-cadherin, which mediates homotypic cell–cell aggregation. (A) The level of N-cadherin, E-cadherin, and  $\beta$ -catenin mRNA of serum-starved HT1080 stable cells was analyzed by semi-quantitative RT-PCR using GAPDH as a control. The lane numbers represent different cell lines as indicated in panel B. The numbers under the N-cadherin RT-PCR gel indicate the normalized quantification of the N-cadherin mRNA transcripts in each cell line. (B) Flow cytometry analysis of the cell surface N-cadherin expression in serum-starved HT1080 stable cells as indicated. MFI: mean fluorescence intensity. (C) Western blot analysis of total cell lysate from the same serum-starved HT1080 stable cells probed by the mAbs as indicated. (D) Cell aggregation assay was performed in the presence of the exogenous reagents as indicated. Data are means  $\pm$  S.E.M. of 3 independent experiments performed in triplicate.

EGTA). As shown in Fig. 4D, both EDTA and EGTA strongly inhibit cell aggregation in all cell lines examined. EDTA plus Mg<sup>2+</sup> partially restores cell aggregation in CD97WT stable cells, but not in other cells. In contrast, EGTA plus Ca<sup>2+</sup> restores cell aggregation fully in all cell lines. This result indicates that the cell aggregation observed herein is indeed Ca<sup>2+</sup>-dependent. Finally, the involvement of N-cadherin in the cell–cell adhesion is confirmed using a blocking anti N-cadherin Ab, which significantly reduces cell aggregation in a dose-dependent manner (Fig. 4D and Supplementary Fig. S4).

In the present report, we have provided strong evidence for a link between the GPS auto-proteolysis and the cellular function of CD97. The establishment of HT1080 stable cell lines expressing CD97 WT and cleavage-deficient (S531A) receptors allows for the systematic evaluation of the functional role of GPS auto-proteolysis (Fig. 1). The comparable expression levels of WT and cleavage-deficient CD97 proteins indicates that GPS cleavage *per se* is not a prerequisite for CD97 receptor trafficking and expression. Instead, our results indicate that GPS cleavage is essential for the formation of a functional CD97 receptor.

The observation that the expression of CD97WT but not CD97S531A isoforms enhanced cell aggregation in HT1080 cells is surprising at first (Fig. 2). As stable cell lines express CD97WT and CD97S531A proteins at a comparable level, it is unlikely the aggregation is mediated directly by CD97 itself. Indeed, our data show that anti-CD97, anti-integrin Abs, and soluble CD97 proteins

all fail to inhibit cell aggregation (Fig. 3). Taken together, these data suggest that the cell aggregation phenotype is induced as a result of the expression of a functional CD97 receptor. The fact that enhanced cell aggregation only occurred when CD97 was properly modified by GPS cleavage indicates its important role in the formation of a functional receptor complex. It is possible GPS auto-proteolysis leads to a conformational alteration of the receptor that activates intracellular signaling events.

Although the nature of intracellular signaling is currently unknown, our data indicate clearly that N-cadherin is one of the target genes induced by CD97 WT proteins (Fig. 4). In addition, some of the adapter proteins of N-cadherin such as  $\beta$ -catenin and  $\alpha$ -catenin are also up-regulated. The resulting effect is the enhanced homotypic cell–cell aggregation. Interestingly, in a recent study using CD97 transgenic mice, specific over-expression of mouse CD97 in enterocytes was shown to up-regulate the expression of  $\beta$ -catenin,  $\alpha$ -catenin, and p120-catenin, which in turn stabilize the structural integrity of E-cadherin-based adherens junctions [33]. As a result, the CD97-transgenic mice are more resistant than WT mice to dextran sodium sulfate-induced colitis.

In conclusion, we demonstrate that expression of CD97 WT isoforms in HT1080 cells up-regulates the expression of N-cadherin and its intracellular adaptor proteins ( $\beta$ -catenin,  $\alpha$ -catenin), which in turn promote Ca<sup>2+</sup>-dependent homotypic cell–cell aggregation. This cellular phenotype requires the expression of a functional

CD97 receptor generated by proper GPS auto-proteolytic modification. As the GPS motif is present in almost all adhesion-GPCRs, our data suggest the GPS auto-proteolysis plays an essential role in the function of adhesion-GPCRs.

## Acknowledgements

This work was supported by Grants from National Science Council (NSC98-2320-B-182-028-MY3) and Chang Gung Memorial Hospital (CMRPD170013 and CMRPD160383) to H.-H. Lin.

## Appendix A. Supplementary data

Supplementary data associated with this article can be found, in the online version, at doi:10.1016/j.febslet.2010.12.005.

## References

- [1] Fredriksson, R., Lagerstrom, M.C., Lundin, L.G. and Schiöth, H.B. (2003) The G-protein-coupled receptors in the human genome form five main families. Phylogenetic analysis, paralogon groups, and fingerprints. *Mol. Pharmacol.* 63, 1256–1272.
- [2] Park, D. et al. (2007) BAI1 is an engulfment receptor for apoptotic cells upstream of the ELMO/Dock180/Rac module. *Nature* 450, 430–434.
- [3] Xu, L., Begum, S., Hearn, J.D. and Hynes, R.O. (2006) GPR56, an atypical G protein-coupled receptor, binds tissue transglutaminase, TG2, and inhibits melanoma tumor growth and metastasis. *Proc. Natl. Acad. Sci. USA* 103, 9023–9028.
- [4] Piao, X. et al. (2004) G protein-coupled receptor-dependent development of human frontal cortex. *Science* 303, 2033–2036.
- [5] Chen, W.S., Antic, D., Matis, M., Logan, C.Y., Povelones, M., Anderson, G.A., Nusse, R. and Axelrod, J.D. (2008) Asymmetric homotypic interactions of the atypical cadherin flamingo mediate intercellular polarity signaling. *Cell* 133, 1093–1105.
- [6] Langenhan, T. et al. (2009) Latrophilin signaling links anterior-posterior tissue polarity and oriented cell divisions in the *C. elegans* embryo. *Dev. Cell* 17, 494–504.
- [7] Weston, M.D., Luijendijk, M.W., Humphrey, K.D., Moller, C. and Kimberling, W.J. (2004) Mutations in the VLGR1 gene implicate G-protein signaling in the pathogenesis of Usher syndrome type II. *Am. J. Hum. Genet.* 74, 357–366.
- [8] Davies, B., Baumann, C., Kirchhoff, C., Ivell, R., Nubbemeyer, R., Habenicht, U.F., Theuring, F. and Gottwald, U. (2004) Targeted deletion of the epididymal receptor HE6 results in fluid dysregulation and male infertility. *Mol. Cell Biol.* 24, 8642–8648.
- [9] Lin, H.H. et al. (2005) The macrophage F4/80 receptor is required for the induction of antigen-specific efferent regulatory T cells in peripheral tolerance. *J. Exp. Med.* 201, 1615–1625.
- [10] Yona, S., Lin, H.H., Siu, W.O., Gordon, S. and Stacey, M. (2008) Adhesion-GPCRs: emerging roles for novel receptors. *Trends Biochem. Sci.* 33, 491–500.
- [11] Lin, H.H., Chang, G.W., Davies, J.Q., Stacey, M., Harris, J. and Gordon, S. (2004) Autocatalytic cleavage of the EMR2 receptor occurs at a conserved G protein-coupled receptor proteolytic site motif. *J. Biol. Chem.* 279, 31823–31832.
- [12] Silva, J.P., Lelianova, V., Hopkins, C., Volynski, K.E. and Ushkaryov, Y. (2009) Functional cross-interaction of the fragments produced by the cleavage of distinct adhesion G-protein-coupled receptors. *J. Biol. Chem.* 284, 6495–6506.
- [13] Volynski, K.E., Silva, J.P., Lelianova, V.G., Atiqur Rahman, M., Hopkins, C. and Ushkaryov, Y.A. (2004) Latrophilin fragments behave as independent proteins that associate and signal on binding of LTX(N4C). *Embo J.* 23, 4423–4433.
- [14] Davies, J.Q., Chang, G.W., Yona, S., Gordon, S., Stacey, M. and Lin, H.H. (2007) The role of receptor oligomerization in modulating the expression and function of leukocyte adhesion-G protein-coupled receptors. *J. Biol. Chem.* 282, 27343–27353.
- [15] Krasnopetrov, V., Lu, Y., Buryanovsky, L., Neubert, T.A., Ichtchenko, K. and Petrenko, A.G. (2002) Post-translational proteolytic processing of the calcium-independent receptor of alpha-latrotoxin (CIRL), a natural chimera of the cell adhesion protein and the G protein-coupled receptor. Role of the G protein-coupled receptor proteolysis site (GPS) motif. *J. Biol. Chem.* 277, 46518–46526.
- [16] Qian, F. et al. (2002) Cleavage of polycystin-1 requires the receptor for egg jelly domain and is disrupted by human autosomal-dominant polycystic kidney disease 1-associated mutations. *Proc. Natl. Acad. Sci. USA* 99, 16981–16986.
- [17] Eichler, W., Aust, G. and Hamann, D. (1994) Characterization of an early activation-dependent antigen on lymphocytes defined by the monoclonal antibody BL-Ac(F2). *Scand. J. Immunol.* 39, 111–115.
- [18] Gray, J.X. et al. (1996) CD97 is a processed, seven-transmembrane, heterodimeric receptor associated with inflammation. *J. Immunol.* 157, 5438–5447.
- [19] Hamann, J. et al. (1995) Expression cloning and chromosomal mapping of the leukocyte activation antigen CD97, a new seven-span transmembrane molecule of the secretion receptor superfamily with an unusual extracellular domain. *J. Immunol.* 155, 1942–1950.
- [20] Aust, G., Steinert, M., Schutz, A., Boltze, C., Wahlbuhl, M., Hamann, J. and Wobus, M. (2002) CD97, but not its closely related EGF-TM7 family member EMR2, is expressed on gastric, pancreatic, and esophageal carcinomas. *Am. J. Clin. Pathol.* 118, 699–707.
- [21] McKnight, A.J. and Gordon, S. (1998) The EGF-TM7 family: unusual structures at the leukocyte surface. *J. Leukoc. Biol.* 63, 271–280.
- [22] Stacey, M., Lin, H.H., Gordon, S. and McKnight, A.J. (2000) LNB-TM7, a group of seven-transmembrane proteins related to family-B G-protein-coupled receptors. *Trends Biochem. Sci.* 25, 284–289.
- [23] Hamann, J., Vogel, B., van Schijndel, G.M. and van Lier, R.A. (1996) The seven-span transmembrane receptor CD97 has a cellular ligand (CD55, DAF). *J. Exp. Med.* 184, 1185–1189.
- [24] Stacey, M., Chang, G.W., Davies, J.Q., Kwakkenbos, M.J., Sanderson, R.D., Hamann, J., Gordon, S. and Lin, H.H. (2003) The epidermal growth factor-like domains of the human EMR2 receptor mediate cell attachment through chondroitin sulfate glycosaminoglycans. *Blood* 102, 2916–2924.
- [25] Wang, T., Ward, Y., Tian, L., Lake, R., Guedez, L., Stetler-Stevenson, W.G. and Kelly, K. (2005) CD97, an adhesion receptor on inflammatory cells, stimulates angiogenesis through binding integrin counterreceptors on endothelial cells. *Blood* 105, 2836–2844.
- [26] Capasso, M., Durrant, L.G., Stacey, M., Gordon, S., Ramage, J. and Spendlove, I. (2006) Costimulation via CD55 on human CD4<sup>+</sup> T cells mediated by CD97. *J. Immunol.* 177, 1070–1077.
- [27] Leemans, J.C., te Velde, A.A., Florquin, S., Bennink, R.J., de Bruin, K., van Lier, R.A., van der Poll, T. and Hamann, J. (2004) The epidermal growth factor-seven transmembrane (EGF-TM7) receptor CD97 is required for neutrophil migration and host defense. *J. Immunol.* 172, 1125–1131.
- [28] Veninga, H. et al. (2008) Analysis of CD97 expression and manipulation: antibody treatment but not gene targeting curtails granulocyte migration. *J. Immunol.* 181, 6574–6583.
- [29] Wang, T. et al. (2007) Improved antibacterial host defense and altered peripheral granulocyte homeostasis in mice lacking the adhesion class G protein receptor CD97. *Infect. Immun.* 75, 1144–1153.
- [30] Galle, J., Sittig, D., Hanisch, I., Wobus, M., Wandel, E., Loeffler, M. and Aust, G. (2006) Individual cell-based models of tumor-environment interactions: multiple effects of CD97 on tumor invasion. *Am. J. Pathol.* 169, 1802–1811.
- [31] Hsiao, C.C., Cheng, K.F., Chen, H.Y., Chou, Y.H., Stacey, M., Chang, G.W. and Lin, H.H. (2009) Site-specific N-glycosylation regulates the GPS auto-proteolysis of CD97. *FEBS Lett.* 583, 3285–3290.
- [32] Pokutta, S. and Weis, W.I. (2007) Structure and mechanism of cadherins and catenins in cell–cell contacts. *Annu. Rev. Cell Dev. Biol.* 23, 237–261.
- [33] Becker, S. et al. (2010) Overexpression of CD97 in intestinal epithelial cells of transgenic mice attenuates colitis by strengthening adherens junctions. *PLoS One* 5, e8507.